IEEE Access
Multidisciplinary | Rapid Review | Open Access Journal

Received March 13, 2020, accepted March 28, 2020, date of publication March 31, 2020, date of current version April 16, 2020.

Digital Object Identifier 10.1109/ACCESS.2020.2984657

A Parametric Optimization Oriented, AFSA Based Random Forest Algorithm: Application to the Detection of Cervical Epithelial Cells

DONGYAO JIA, (Senior Member, IEEE), ZHENGYI LI, AND CHUANWANG ZHANG
School of Electronics and Information Engineering, Beijing Jiaotong University, Beijing 100044, China
Corresponding author: Chuanwang Zhang (cwzhang1995@qq.com)

ABSTRACT Cervical cancer is one of the most common cancers among women in the world, over 570,000 patients are affected annually. Pathological examination for patients using Pap Smear becomes the mainstream of cervical cancer diagnoses. Accurate diagnoses and analyses largely rely on 3 factors: cell segmentation, feature extraction and selection as well as classification. Firstly, a 2-layer segmentation algorithm based on block Maximum Between-Class Variance (Otsu) and Gradient Vector Flow (GVF) Snake model is applied to obtain regions of interest (ROI). Then the features of chroma, shape and texture are extracted and selected for a better classification performance. The random forest algorithm based on Artificial Fish Swarms Algorithm (AFSA) is used to recognize and classify cervical epithelial cells. The proposed methods were tested on 200 cervical Pap Smear images. Experimental results show that cervical cells can be segmented with an effective segmentation result. The proposed feature selection method achieved an accuracy of 81.31% with the minimum feature number. The improved random forest algorithm with 2 and 7 classification under fivefold cross-validation reaches the highest classification accuracy (96.86%). Experimental results showed that the proposed method has obvious recognition advantages, and thus provides a practical classification frame for the diagnoses of cervical cancer.

INDEX TERMS Artificial fish swarm algorithm, random forest, cell detection, image segmentation.

I. INTRODUCTION

As we all know, the incidence rate of cervical cancer in gynecological tumors is just lower than breast cancer, which is exactly a female killer. More than 270000 women died of cervical cancer each year all around the world, most of which occurred in developing countries [1]. Detection and screening of cervical cancer in developing countries are encountering severe problems due to the sanitation and economic conditions. The incidence of cervical cancer in the developing countries is a lot higher than that in developed countries. As for China, there are about 130,000 new cases of cervical cancer every year, occupying 28% of the world's total number [2]. In the United States, it was counted that 13,240 new cases of cervical cancer were diagnosed in 2018 with a death number of 4170 [3]. Therefore, the grim reality leads to an urgent need for appropriate methods on the cervical cancer detection and identification.

The associate editor coordinating the review of this manuscript and approving it for publication was Muhammad E. H. Chowdhury.

There exists a strong correlation between the disposing time and the prognosis of cervical cancer. The earlier the cervical cancer is treated, the better the therapeutic effect will be. Only the early detection of cervical cancer is achieved, the early intervention can be applied. The basic requirement of early detection is that women takes physical examination annually. According to the prediction of relevant research institutes, if the cervical cancer screening is implemented at early stage, the cure rate for cervical cancer can reach 90-92% [4]. However, due to the large population of reproductive age women in different countries around the world, and the corresponding small number of medical institutions and experienced pathologists, the treatment of regular cervical cancer screening has resulted in a realistic contradiction, which is the goal of regular cervical cancer screening cannot be met.

Cervical cancer is traditionally diagnosed by using liquid-based cell slides, under the supervision of pathologists, which makes the diagnoses largely depend on the doctors' subjective experience. However, the number of pathologists with rich

experience is relatively small, and their work efficiency and diagnostic accuracy are largely affected by working hours, so there are still insufficient pathologists compared with the whole population of potential patients [5]. World Health Organization (WHO) regards the number of doctors in every 1,000 people as an important criterion to measure the national healthy level [6]. That number in China was only 2.4 in 2013, just about half of the number in developed countries during the same period [7]. On account of the huge gap between the need of patients and the number of doctors, many cervical cancer patients cannot get timely and effective diagnoses as well as treatments, which seriously affects their quality of life. Therefore, the emergence of efficient computer-aided cervical cancer diagnosis system with high accuracy describes a possible approach to solve this problem, which is what we are working on.

Traditional methods of diagnoses based on liquid-based cell slides have played an important role in the past few years, it saved many women's lives. But it also carries the high prices and dependence on pathologists' experience. These problems also lead to the decline of accuracy on testing methods and false positive or false negative rates [8].

Besides, there are other methods used for the clinical application of cervical epithelial cells recognition, such as Pap Smear and acetic acid experiment [9]. They heavily rely on subjective experience of pathologists, who need to observe cells directly through microscopes, which is difficult for doctors to concentrate on observing for a long time. The information obtained from acetic acid experiments is quite simple and the accuracy rate is not better than the artificial extracted features.

In the detection of cervical cancer, the main object of the study are usually cervical epithelial cells, which are known to play a crucial role in the innate and adaptive initiation, maintenance, regulation in several tissues [10]. So that automatic methods focusing on cervical epithelial cells have been widely applied to detect abnormal cells from liquid-based cell slides by analyzing the contours of the cells [11]. In recent years, the methods of automatic analysis of cervical cell images have been developed and improved. In the methods mentioned above, cells are put onto the liquid-based slides, images of slides are then captured by industrial cameras. Abnormal cells are obtained by analyzing pictures, by which different cells are also classified. This method greatly reduces the working pressure and error rate of pathologists, improves the efficiency and accuracy of detection, and has a great capacity in practical application. Three keys of this method are cell segmentation, feature extraction and classification. In the following lines, these three parts have been elaborated. For easy understanding, we summarized the main works in this field in recent years in Table 1.

Traditional solution to segmentation problems only applied for free-lying cells. Most methods of segmenting cells form the background mainly based on simple image histogram threshold approaches. Like optical density information [12], compactness information [13] and grey level brightness [14].

TABLE 1. Advantages and limitations of methods reviewed in this paper.

Methods	Advantages	Limitations
Segmentation		
Threshold method	High computational efficiency	Bad for images without obvious difference in gray level
Watershed	Fast speed and good robustness	Excessive segmentation
Edge detection algorithm	Good on the edges	Cannot get good region structures
Gradient Vector Flow (GVF)	Automatic and adaptive	Sensitive to initial position
Graph-based method	Fast speed	Easy to over segmentation
Feature extraction		
Multidimensional feature extraction	High accuracy	Large computation
Area, integrated optical density (IOD) and compactness	Simple calculation	Subject to light
Nuclear gray level, area of cytoplasm	Simple calculation	Subject to accurate edge
Contrast, mean intensity and correlation	Good anti-noise performance	Only reflects properties of surface
Multi-spectral texture feature extraction	High accuracy	Common speed
Spectral information obtained by Fourier transform	Hight accuracy	Large computation
Classification		
Support Vector Machine (SVM)	Easy to control	Training speed is slow
Artificial Neural Network (ANN)	Good anti-noise performance	Easy to be overfitting
k-Nearest Neighbor (kNN)	Robust and fast speed	Complexity increases as attributes
Random forest	Easy to understand	Error in training will lead to bad results
Convolutional Neural Networks (CNN)	High accuracy	Large computation

The key point of these methods is to find the optimal threshold [15]. These works contribute greatly to cell image domain while still exist room for improvement. As time flies into 2011, Plissiti *et al.* [16] applied watershed based on shape prior and artifact removal using distance-dependence rule for computation, which achieved a good segmentation effect.

Edge detection algorithm removes the requirement of prior knowledge, methods like morphological processes [17], color clustering [18], Sobel operators, or non-maximum suppression [19] were carried out successively. However, these methods are not suitable to be used individually for images with poor contrast or overlapping cells. Snake (2D) model was utilized by Bamford and Lovell [20] in a Viterbi search-based dual active contour algorithm. Besides, the Gradient Vector Flow (GVF) model was used for the estimation of cell nuclei [21]. Graph-based method was also employed by Zhang *et al.* [22] to achieve the nucleus segmentation. Examples including SVM [23] or Gaussian mixture model [24] were also introduced to the field of cell segmentation. Nowadays, more and more machine learning cell segmentation algorithms have been developed and occupied an important position in this field.

As for the cell feature extraction, most researchers applied multidimensional features to identify the cells [25]. Some scholars turned to features like area, integrated optical density (IOD) and compactness [26]. Other scholars used several features: nuclear gray level, area of cytoplasm and so on [27]. Besides, some researchers took contrast, mean intensity and correlation as selected features for classification [25]. The feature extraction method based on signal processing in cell image is established according to the target point, then the corresponding features are extracted. This method is intuitive and simple [28]. Some researchers have proposed new feature extraction methods for cervical cell images: Zhangjiayong and Liuyanxi proposed a multi-spectral texture feature extraction method, which can effectively identify cancer cells [29]. Chankong used the spectral information obtained by Fourier transform to extract the features of normal and abnormal cells [30]. However, at present, most of the feature extraction methods are based on the accurate segmentation of the nucleus, which are used as auxiliary roles with the other methods.

In regards to the cervical epithelial cell classification algorithms, feature-based machine learning algorithms are mostly applied for classification targets, and in recent years, deep learning approaches have also developed. In a study by Huang *et al.* and Chen *et al.* [31], the researchers applied support vector machine (SVM) to cervical cells. Artificial neural networks (ANN) was implemented for cell classification by Mango [32] as one of the most popular classification techniques. As for supervised methods, k-Nearest Neighbors (k-NN) was integrated with fuzzy intuition and achieved feature selection by combining with a quantum-behaved particle swarm optimization by Marinakis *et al.* [33]. The RBF-SVM also obtained a good result in a study by Bora *et al.* [34]. Besides, Jie *et al.* [35] proposed a two-level classification system for the automatic detection of cervical cancer cells. Zhao *et al.* [36] introduced feature quantization method to detect the cervical squamous epithelial cells and achieved good results. Some other methods for detecting cervical lesions can also be tried in the classification of cervical epithelial cells, for example, semantic image analysis proposed by Park *et al.* [37], structural analysis of histological images on detecting cervical cancer by Miranda *et al.* [38], as well as the protein detection on the classification of cells applied by Volgareva *et al.* [39]. As for deep learning methods, comparison-based CNN for cervical cells detection by Liang *et al.* [40] and deep belief network verified by Rasche *et al.* [41] achieved higher accuracy when compared to a traditional methodology in segmentation and feature extraction.

From these pioneer studies, it is known that the method of classifier integration and special parameter optimization could help to enhance the sensibility and specificity comparing to the traditional classifiers. Especially the proposed random forest algorithm, which is not only applied for traditional classification task, but also used for deep learning relevant missions like combining with cascade of deep learning to detect masses in mammograms [42], integrating with deep learning to build a computational imaging framework for reliable detection of blood vessels [43], being grown on convolutional neural networks for scene categorization [44]. Comparing to it, traditional cell segmentation and classification methods cannot effectively segment or classify the cervical epithelial cells, the reliability and accuracy of diagnosis results are often restricted, which seriously hinders the detection of cervical epithelial cells.

In order to deal with the challenges in both biology and computation that decreased the effect of recognition, we proposed an improved random forest algorithm for cervical epithelial cell detection in this paper, which contains 3 major parts: (1) Cell segmentation: block Otsu algorithm for the first segmentation and GVF Snake model for the second segmentation. (2) Feature extraction and selection: take advantage of the AFSA algorithm to optimize the feature selection. (3) Classification: improved random forest algorithm based on AFSA is used to reduce the time cost and improve the classification performance, also the robustness and generalization ability of classification enhanced. The workflow of the proposed method is as shown in Figure 1.

This paper is divided into 7 sections. Section **I** presents a review of the methods for cervical cell segmentation, feature extraction and classification. Section **II** describes the data source and the acquisition process of the images used for analyzing. Section **III, IV and V** presents the methods in image segmentation, feature extraction and classification. Section **VI** conducts the experiments and analysis the results. Finally, conclusions are drawn in Section **VII.**

II. MATERIAL

A. CELL MATERIAL

Pap Smear images for this study were obtained at Guangdong Province People's Hospital, Guangdong, China, which is our cooperative medical institution. Experienced doctors and pathologists collected the samples from 200 patients and prepared the liquid-based cell slides, whose sensitive information have been removed, including name, phone number, etc. The processing and staining of Pap Smear were conducted at their laboratories. Samples were collected from patients

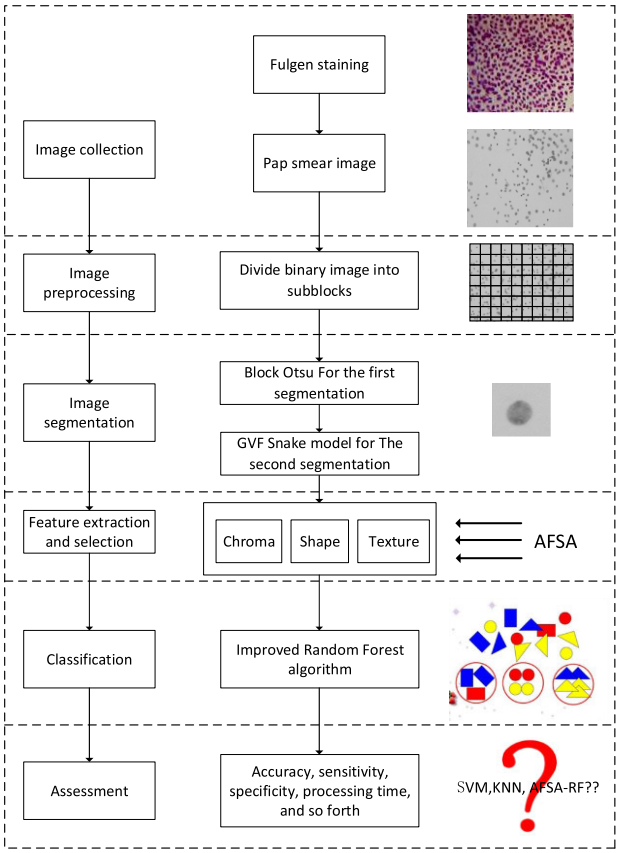

FIGURE 1. Pipeline of the proposed method.

following all ethical stipulations, all the materials will only be used for medical purpose.

Images used in this paper are captured through industrial camera (DFK33G274, Imaging source) using 400x resolution and 24bits color depth, 3-dimensional electric platform (OptiScan III, Prior Scientific), Twentyfold magnifying industrial microscope (DM3000, Leica). 30 images were captured from each slide. Then digitized images were reviewed by experienced pathologists to obtain the 20 best images, which indicates that the smear level database contains 4000 images (200 patients and 20 images each patient). The original corresponding reports from the hospital were also obtained in order to label the images. After cell segmentation the most representative 800 cell images were picked out according to pathological criteria for use of the proposed method. These cells were made by a new Pap Smear technique, which are divided into 7 subclasses by judgment of pathologist. Image details are shown in Table 2.

More detailed cell category data is shown in Figure 2, all of which were annotated by the pathologists from the cooperating units, whose accuracy has been guaranteed. Detailed data refers to 7 kinds including superficial squamous (32), intermediate squamous (35), columnar (45), mild dysplasia (76), moderate dysplasia (61), severe dysplasia (78), and carcinoma in situ (73).

TABLE 2. Details of the obtained images.

Generated database: Smear level	Number	Details
Normal	60	Resolution:400x
Cancerous	140	Size: 1200x1600,1300kb
Generated database: Cell level	**Number**	**Details**
lymphocyte	400	Resolution:400x
Normal epithelial	200	Size: 70x70, 8kb
Cancerous epithelial	200	

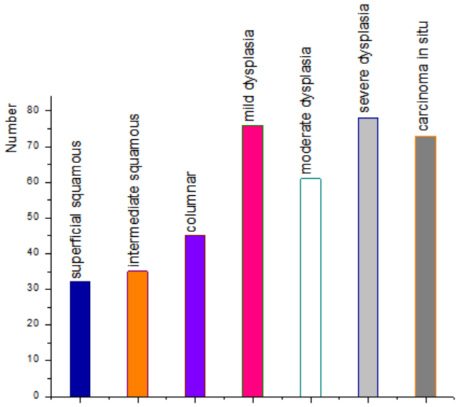

FIGURE 2. Schematic diagram of cell type distribution.

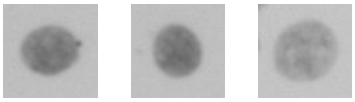

FIGURE 3. Main shapes of cell images after segmentation.

The pixel size of cell image after segmentation is 70 × 70, and the physical size is about 8kb. The color is gray, and the image depth depends on the amount of DNA in nucleus. The shape of the cell image is round or elliptic, and a small amount of them are close to irregular shape. For the sake of illustration, main shapes of cells are displayed in Figure 3.

III. IMAGE SEGMENTATION

Due to multiple limitations and difficulties in the process of smear making and image acquisition, there are always decreases in quality like uneven staining, noise during processing, which increase the difficulty for accurate image segmentation. Cell image segmentation plays an important role in the automatic cell classification, which determines the accuracy of features and robustness of the system. Block Otsu and GVF Snake model are introduced as an effective method in this paper, which is not only simple in calculation, but also practical in dealing with images with complicated backgrounds. Block Otsu is firstly applied to make rough

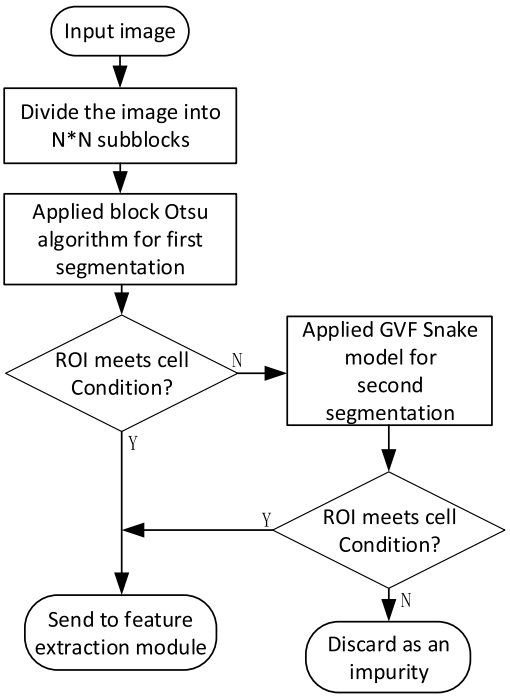

FIGURE 4. Flow chart of image segmentation algorithm based on Otsu and GVF Snake model.

segmentation of cell image, after which the image of single cell is obtained, whose shape can be tested using the conditions below:

(1) Area test. Whether the number of pixels Np in ROI stays in range of [N min, N max], which indicates the normal cell area.

(2) Deformity test. The deformity degree of the ROI area is calculated by deformability calculation equation$\gamma = l/Np$, the l in the equation stands for the perimeter of ROI. Deformity threshold value is γT, and the condition is satisfied when $\gamma \leq \gamma T$.

If the test conditions above are satisfied, ROIs will be determined as the cell image and then put into the feature extraction module. If the ROIs do not pass the test, they will be segmented a second time by the method based on GVF Snake model. Then shape of the second segmentation result is tested using the same test conditions. The ROI will be judged as impurity and discarded directly if the condition is not satisfied again. The other ROIs passed the test will be determined as cell images and extracted features. Flow chart of the image segmentation algorithm is as shown in Figure 4.

A. ROUGH SEGMENTATION BASED ON BLOCK OTSU ALGORITHM

The core idea of Otsu algorithm can be expressed as equation (1). Assuming that the threshold between foreground and background is K, the optimal choice of K should satisfy the variance σ_B^2.

$$\begin{cases} \sigma_B^2 = \omega_1 (\mu_1 - \mu_T)^2 + \omega_2 (\mu_2 - \mu_T)^2 \\ \rho_r (r_q) = \dfrac{n_q}{n} \\ \omega_1 = \sum_{q=0}^{K-1} p_q (r_q) \\ \omega_2 = \sum_{q=K}^{L-1} p_q (r_q) \\ \mu_1 = \dfrac{\sum_{q=0}^{K-1} q p_q(r_p)}{\omega_1} \\ \mu_2 = \dfrac{\sum_{q=K}^{L-1} q p_q(r_p)}{\omega_2} \\ \mu_T = \sum_{q=0}^{L-1} q p_q(r_q) \end{cases} \tag{1}$$

In the formula, n stands for the total number of the pixels in the image. L indicates the total number of gray levels in the whole image, and nq is the number of pixels with a gray level of rq, $q = 0, 1, 2, \cdots L-1$. Foreground pixels in the image belong to set $C_1$with a value range of $[0, 1, \cdots K-1]$; background pixels belong to set $C2$ with a value range of$[K, K+1, \cdots L-1]$.

Since the uneven illumination and cell overlapping situations in practical production, which will affect the classification accuracy of cervical cells. This paper chooses the block Otsu algorithm to segment the image and divide to subblocks. In the end the whole image is combined by the block sequence [45].

Main steps of block Otsu algorithm are as shown in Figure 5.

B. SECOND SEGMENTATION BASED ON GVF SNAKE MODEL

1) TRADITIONAL SNAKE MODEL

Snake model is also called as Active Contour Model (ACM), whose main idea is to minimize the energy of whole system. That is to say that the initial closed contour curve is depended on the periphery of the target, which is described by energy function. The energy function can be solved under certain approximation rules. So that the initial contour curve will approach and finally converge to the target edge [46]. At this point, the energy value of the curve also represents the energy functional value, which has reached the minimum. Specific process is defined as follows:

First, we need to define the initial closed contour curve around the target edge, in addition the energy function of the curve is expressed as equation (2).

$$E_{snake} = \int_0^1 E_{internal} + E_{external} ds \tag{2}$$

$$E_{internal} = \frac{1}{2}\left[\partial (s) \left|x' (s)\right|^2 + \beta (s) \left|x'' (s)\right|^2\right] \tag{3}$$

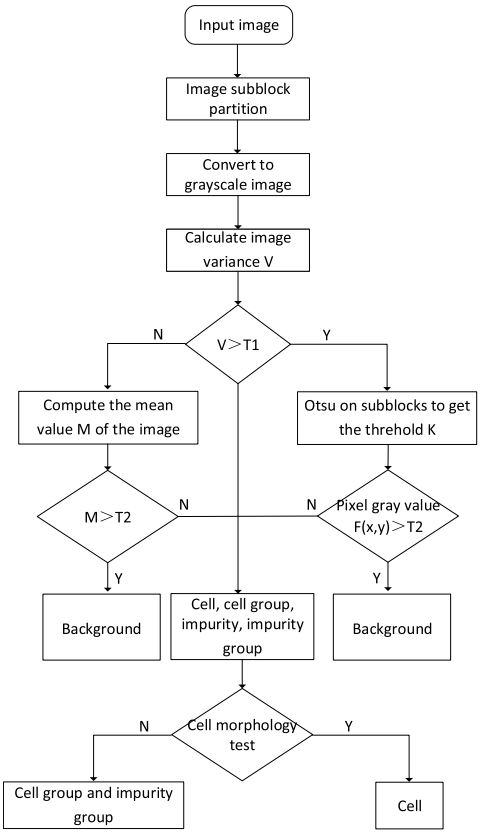

FIGURE 5. Flow chart of image segmentation algorithm based on block Otsu.

$$E_{external} = E_{ext}\left(x\left(s\right)\right) \tag{4}$$

In equation (3), *Einternal* stands for the internal energy. The other two terms in the definition are the first and second derivative of the curve, representing the slope rate of pixels on the curve and the curvature of the points. These two terms can keep the curve continued and smooth when the curve approaches the target curve. Among which, $\partial(s)$ represents the elastic coefficient of the curve. The curve will generate a breakpoint when $\partial(s) = 0.\beta(s)$ stands for the rigidity coefficient of the curve. The curve may generate a corner point when $\beta(s) = 0$. Generally speaking, $\partial(s)$ and $\beta(s)$ are usually set as constants for the sake of simplicity.

As for equation (4), *Eexternal* indicates the external energy, whose value has strong relations with the local information of the image. *Eexternal* can make the curve approach to the target curve continuously, and its concrete value calculation is defined as follows:

$$E_{external} = E_{ext}\left(x\left(s\right)\right) = -\left|\nabla I\left(x, y\right)\right|^2 \tag{5}$$

Or,

$$E_{external} = E_{ext}\left(x\left(s\right)\right) = -\left|\nabla\left(G_\sigma\left(x, y\right) * I\left(x, y\right)\right)\right|^2 \tag{6}$$

Among which, $G\sigma$ is the standard deviation of Gauss function, $I(x, y)$ is the original graph, and ∇ stands for the gradient operator.

TABLE 3. Feature to be extracted.

	Features
Chroma	Average value of three channels: AR, AG, AB
	Standard deviation of three channels: SR, SG, SB
	Deviation of three channels: VCR, VCG, VCB
Shape	Area, perimeter, roundness, rectangles
Texture	Contrast, energy, entropy, homogeneity

In order to make the preset contour curve coincide with the target edge, which means, the energy function *Esnake* can be minimized if it satisfies the following Euler equation (7):

$$\frac{\partial}{\partial s}\left(\alpha\left(s\right)\frac{\partial x\left(s\right)}{\partial s}\right) - \frac{\partial^2}{\partial s^2}\left(\beta\left(s\right)\frac{\partial^2 x\left(s\right)}{\partial s^2}\right) - \nabla E_{ext}\left(x\left(s\right)\right) = 0 \tag{7}$$

2) GVF SNAKE MODEL

GVF Snake model uses the gradient vector flow (GVF) instead of the Gauss potential field from the traditional model. Besides, its mathematical calculation is based on the Helmholtz theorem in the electromagnetic field. GVF field of the GVF Snake model is shown as equation (8).

$$F_{ext}^{(g)} = V\left(x, y\right) \tag{8}$$

As is shown above, the external energy *Eexternal* in equation (2) is replaced by that of equation (8).

Compared with Gauss potential field, GVF field obtains the gradient vector of the whole image. By which the external force field has a wider range of action. It also means that even if the selected initial contour is a little far away from the target contour, it will converge to the target contour adaptively. At the same time, the external force acting on the concave part of the target contour will increase as the external force scope increases, so that the boundary can converge to the concave part as we supposed [47].

IV. FEATURE EXTRACTION

A. BASIC FEATURES TO BE EXTRACTED

Selection of cell features plays an essential role in cell classification. Contamination of cervical cells like lymphoid and junk cells always exist. According to prior knowledge of cell feature extraction, the features of cervix exfoliated cells are extracted from the aspects of chroma, shape and texture. Specific extracted features are as shown in Table 3. From the data in table, it is concluded that there are 11 features to be selected, among which the chroma feature has the color component of three channels, all the features of different channels are denoted as the same one.

B. FEATURE EXTRACTION OF CELL IMAGES

The construction process of random forest algorithm is mainly divided into 3 parts: feature extraction on training set, training and execution of decision tree [48]. The size of forest and the subset size of attributes are important parameters that we focus in training process [49].

The larger *nTree*is, the more decision trees in the random forest there will be. Besides, the diversity of random forest classifier will be richer, which also contributes to the classification accuracy. While when *nTree* reaches a certain value, the classification effect tends to be constant, meanwhile the cost of the classifier is larger and the interpretability will decrease. If *nTree* is set to be too small, the diversity of classifiers will be worse, and the classification performance will also be poor with a lower accuracy rate. The parameter k stands for the size of the subset in the random forest when the nodes are splitted and sampled from the entire feature set. In general, the value k remains unchanged since the decision tree is created, and it is far smaller than the size of the total feature set. The impact of k is to prevent the classifier from overfitting and increase the diversity. If the value k becomes too large, the diversity of the decision tree will decrease and the classification effect is also reduced. While when the value k is set too small, the diversity of base classifiers will reach a higher level, meanwhile the classification accuracy and the generalization ability of the classifier will decrease.

V. RANDOM FOREST MODEL BASED ON ARTIFICIAL FISH SWARM OPTIMIZATION

A. FEATURE SELECTION AND PARAMETER OPTIMIZATION MODEL BASED ON AFSA

Integrated classifiers are the choice of many researchers nowadays in fields like bioinformatics, which also indicates that a higher classification accuracy will be obtained if the base classifier achieves an ideal result and does not affect each other [50]. Therefore, when the random forest model needs to be improved, one practicable way is to improve the classification accuracy of the single decision tree as much as possible, meanwhile keeping each tree separated.

Aiming at the optimization of random forest classifier, the model based on artificial fish swarm algorithm is proposed in this paper, which applies the artificial fish swarm algorithm to select the features of the random forest classifier and optimize the parameters from the forest scale. The artificial fish swarm algorithm behaves well in overcoming the partial extremum and obtaining the global extreme point. Only the value of target function is applied for the algorithm, the special information including gradient value which is also available to the searching space will be excluded. Besides, the algorithm is not sensitive to the initial value as well as the selection parameters, which is exactly useful for the optimization [51] of the parameters of the random forest algorithm. In a word, the artificial fish swarm algorithm is introduced to optimize the model due to the above advantages.

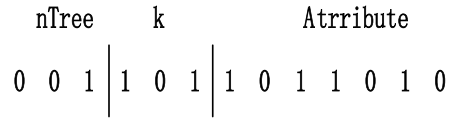

FIGURE 6. Binary coded schematic diagram.

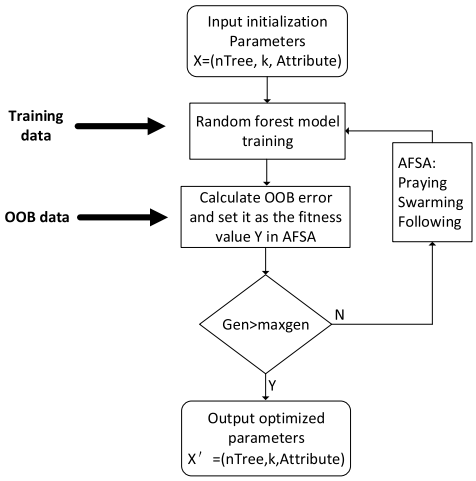

FIGURE 7. Flow chart of random forest model parameter optimization based on AFSA.

Traversing the k through p-fold cross-validation is applied to solve the optimal value, which is calculated according to the minimum error value or the maximum Area Under Curve (AUC). However, the time complexity of this algorithm stays at a high level, which determines that it is not suitable for the feature set of large data. Since the approach of parameter optimization is minimizing the generalization error, two classification data can use Out of bag (OOB) error to replace the time consumption of cross validation during the following feature selection and parameter optimization process. As for the process of classification, cross validation is necessary. Feature selection and optimization are conducted as follows:

Variables that need to be optimized:

$$nTree, k, \{Attributei|i = 1, 2, \cdots, M\}$$

Objective function:

$$f(nTree*, k*, \{Attributei|i = 1, 2, \cdots M\}) = \arg\min(avg(OOBerror)) \quad (9)$$

The range of initial value for *nTree* is $[0, 500]$, and the range for k is $[1, M]$. During the computing process of artificial fish swarm algorithm, the state variables are all binary coded. All the numbers are divided into 3 segments when coding, and the schematic diagram is shown in Figure 6. The original numbers of *nTree* and k are binary coded and placed on the first 2 segments respectively. 0 for the $\{Attributei|i = 1, 2, \cdots, M\}$ section indicates that the located feature is not chosen, and 1 indicates that the located feature is selected. And there consistently exists a constraint $k \leq sum(Attributei = 1)$. Applying the above feature selection method, features meet the requirements will be selected. In the subsequent classification and comparison experiment, feature selection method proposed in this

TABLE 4. Calculating steps for AFSA.

Algorithm: Random forest based on AFSA	
1	Initialize the parameters of AFSA and RF algorithms: (numbers of iteration, artificial fish, location of fish, visual field of fish, maximum step length, crowding degree factor, maximum number of behavior attempts, size of the random forest scale, the attribute subset size)
2	The original training set is (X, Y) $(x_1, y_1), (x_2, y_2), \cdots (x_N, y_N) \in (X, Y)$,the number of the listed sets is N .Bootstrap sampling method randomly extract N samples (x_i, y_i) as training samples (X^*, Y^*)
3	Input training sample (X^*, Y^*) ,select k feature subsets when tree splits while training the decision tree
4	Loop the 2,3 above until the decision tree forest with preset number $nTree$ is generated, meanwhile, the initial establishment of the random forest classifier is completed
5	OOB sample is used as a test sample to test the classifier. Then the OOB error is obtained and used as the fitness value Y for the AFSA algorithm
6	Judge whether $gen > Maxgen$ is achieved: if is, output the RF classifier parameter $nTree$, k , $\{Attribute_i \mid i = 1, 2, \cdots, M\}$ and enter 8; otherwise, set the RF classifier parameter $X = \{nTree, k, Attribute\}$ as the initial state of the artificial fish to forage, cluster and tailgate, then update the global optimal artificial fish state $X' = \{nTree, k, Attribute\}$
7	Use the optimized parameters $X' = \{nTree, k, Attribute\}$ to reset the RF classifier and enter 2
8	Finish the training of the classifier and keep OOB error as the correct rate of classification λ

paper will be compared with other similar methods, aiming at demonstrating the superiority of the method based on AFSA.

The flow chart of feature selection and parameter optimization based on fish swarm algorithm is as shown in Figure 7.

B. EPITHELIAL CELL RECOGNITION BASED ON IMPROVED RANDOM FOREST ALGORITHM

According to the theoretical analysis above and model establishment, the improved random forest classifier for epithelial cell recognition will be trained as follows in Table 4:

Flow chart of the epithelial cell recognition algorithm based on the improved random forest model is as shown in Figure 8.

VI. EXPERIMENTAL VERIFICATION AND ANALYSIS

A. IMAGE SEGMENTATION EXPERIMENT

1) EXPERIMENTS AND RESULTS

Figure 9 stands the segmentation process of a cervical cell image. Graph (a) is the original image. Graph (b) is a binary

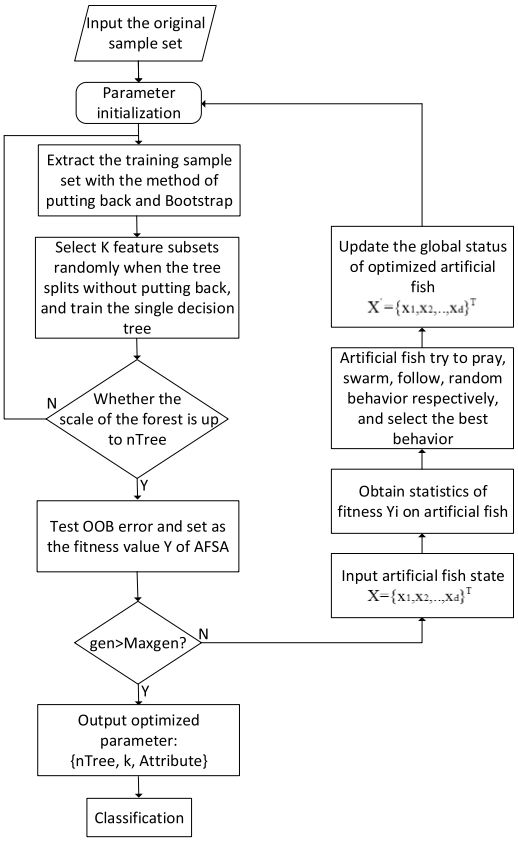

FIGURE 8. Flow chart of cervical epithelial cell recognition algorithm based on improved random forest model.

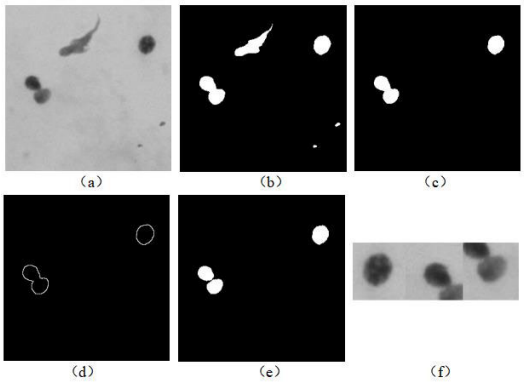

FIGURE 9. Segmentation of cervical cell image based on block Otsu and GVF Snake algorithm.

image divided by block Otsu algorithm. By comparing the graph (a) and (b), background and foreground of the image are segmented better, meanwhile some impurities are also separated as the foreground. Figure (c) stands for the binary picture after shape test, which is handled by the area and deformity test according to III (1), (2). Through the image comparison it is concluded that areas which dissatisfy the screening conditions or ROIs with high rate of deformity (which are impurities) are eliminated by the morphological testing method. Graph (d) expresses the edge detection result

TABLE 5. Segmentation accuracy between different methods.

Method	Pixel classification accuracy
GVF	0.8847±0.0449
Proposed method	**0.9153±0.0506**

of (c), which is obtained by Canny edge detection algorithm. Its purpose is to define the initial contour closed curve for GVF Snake model. Graph (e) is an image of binary result generated by GVF Snake model. Since the Snake model is based on the solution of the energy function to calculate the initial contour curve while approaching the edge of target, the improved GVF Snake model behaves better on the edge convergence of the concave shape. Besides, it can be indicated by the contrast of (c) and (e) that cells close to together are accurately separated. Graph (f) is the final foreground image which has been segmented totally. As is shown, the result is better rid of the interference pixels such as impurities, which shows ideal outcome.

2) COMPARISON OF METHODS IN IMAGE SEGMENTATION

The purpose of this section focuses on illustrating the improvement made by the proposed Otsu and GVF Snake model. Based on the data introduced in Table 2, comparative experiments were carried out. 78 cervical cell images are chosen from our own dataset. Performances of different models are evaluated by calculating the ratio of correct divided pixels to all pixels, in which the professional software Image-J was applied. Statistical results are shown in Table 5. Table 6 compares some segmentation results by GVF and method from this paper.

From Table 5 and 6, we can see that the method proposed in this paper performs better than GVF in locating true edges of images. The proposed method is more robust and able to successfully estimate the true boundaries in cases above. It is concluded that the method of Otsu-GVF Snake model shows an improvement in the segment of cells.

3) BIOLOGICAL INSIGHTS GAINED BY THE NEW METHOD OF IMAGE SEGMENTATION

Based on the image segmentation experiment it can be concluded that the fuzzy boundary in the traditional cervical cell picture has been improved significantly after the treatment of binary division and corrosion. Besides, overlapping cells which are not easy to observe and analyze have been effectively separated. Impurities and irregular shapes have been removed by our method including Otsu, shape detection and GVF Snake model. The proposed method does not strictly require initial pixel selection, which is also an advantage in the field of cell segmentation.

TABLE 6. Segmentation results between different methods.

No.	Original	GVF	**This paper**
1	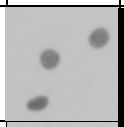	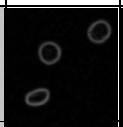	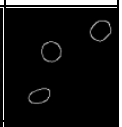
2			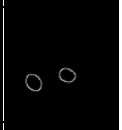
3	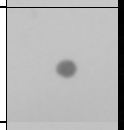	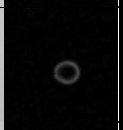	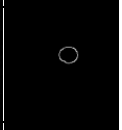
4	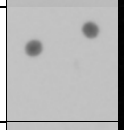	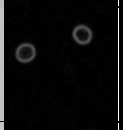	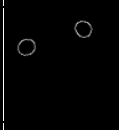
5	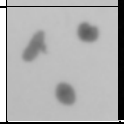	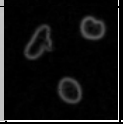	

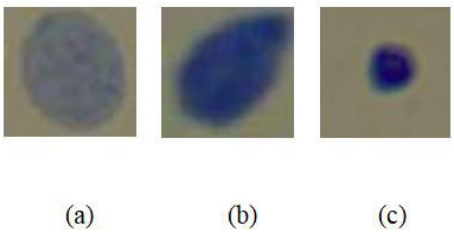

(a) (b) (c)

FIGURE 10. Cell images used in feature extraction experiment.

B. EXPERIMENT OF FEATURE EXTRACTION

Cell images are separated completely from each other after the experiment above. Later features of chroma, shape and texture will be extracted from the images in this part. On account of the parameter sensitivity problem, an ensembled method is applied to extract several influential parameters which contribute in cell classification. The experimental images are as shown in Figure 10.

1) EXPERIMENT OF CHROMA EXTRACTION

Average value of three channels AR, AG, AB, variance SR, SG, SB, deviation VCR, VCG and VCB were extracted respectively. Feature values are shown in Table 7.

It is concluded that B color channel has a higher mean value and a lower variance as well as deviation, which indicates that component of B color occupies a relatively high proportion in the whole color space. Moreover, B color components are uniform and the pixel value is less random. Therefore, B channel is determined as the most representative one from the other two.

TABLE 7. Samples of chroma features.

Cell	a	b	c
AR	114.9	82.4	69.5
AG	114.7	90.4	71.5
AB	127.0	103.1	98.6
SR	16.8	38.0	39.9
SG	13.4	31.7	38.6
SB	4.2	5.4	9.8
VCR	53.0	112.4	118.2
VCG	48.3	95.6	115.7
VCB	9.2	16.9	29.1

FIGURE 11. Binary cell images of feature extraction experiment.

TABLE 8. Samples of shape features.

Cell	Area	PERI	Round	RECT
a	1573	130	0.59	0.89
b	1152	114	0.55	0.72
c	504	71	0.54	0.83

After determining the color channel, feature parameters under the same color channel can be obtained by applying the feature selection method based on AFSA in this paper.

2) EXPERIMENT OF SHAPE FEATURE EXTRACTION

In order to accurately coordinate the ROI, images in Figure 11 are first processed by binary processing, later the statistical shape features are extracted as shown in Table 8.

As is indicated from the data in Table 8, the specific performance of different parameters of the three cells in the example is shown. Based on the statistical results of all the cells, area, perimeter and roundness have higher mean value and lower standard deviation comparing with other features. In the AFSA feature selection, all three parameters mentioned above were selected and left.

3) TEXTURE FEATURE EXTRACTION

Take cell images in Figure 10 as the sample for texture feature extraction. Contrast, energy, entropy and homogeneity of cells (a), (b) and (c) in Figure 10 are calculated and then shown in Table 9.

We can conclude that the distribution of elements in cell a is more dispersed according to the texture feature values in Table 9, comparing with cell (a) and (b). When the contrast and homogeneity show larger, the cell edges are more obvious and the inner texture is coarser. According to the above AFSA feature selection algorithm, energy, entropy in the texture features are selected to remain.

TABLE 9. Experimental nuclear texture features.

Cell	CON	ENE	ENT	HOM
a	1.02502	0.03290	3.65927	0.48803
b	1.24796	0.05717	3.40372	0.56347
c	1.48325	0.05337	3.28106	0.53726

TABLE 10. Feature selection algorithm comparison.

Algorithm	Accuracy (%)	Number of features
Literature [51]	79.34	11
Literature [52]	80.92	11
Literature [53]	76.67	9
Literature [54]	79.58	9
Proposed method	**81.31**	**7**

To sum up, among all the features, 7 of which, average, variance, area, perimeter, roundness, energy and entropy are retained according to the feature selection method based on AFSA.

4) COMPARISON OF FEATURE SELECTION METHODS

In order to illustrate the effectiveness of the feature selection method in this paper, we adopted an experimental scheme which keep the classifier fixed while making the feature selection method change. The classifier adopts the random forest classifier based on AFSA proposed in this paper, feature selection methods applied for the experiment are as shown in Table 10, epithelial cells were used as the classification data. Through the experimental method of controlling variables, we can obtain the quantitative indicators like accuracy under different feature selection methods to judge whether the proposed method in this paper has certain superiority.

Literature [52] collected a total of 121 features comprising 5 shape descriptor, 50 textures, 66 ripplet descriptors and applied an ensemble classification using weighted majority voting. Literature [53] divided the image into blocks with certain size and extracted the texture and color histogram features which show significant differences between blocks with and without suspicious cells, then these features are input into the support vector machine for classification. Literature [54] used Radiating Gradient Vector Flow Snake to segment the single cervical image into cytoplasm, nucleus and background, then cellular and nuclei features are extracted for the training of Support Vector Machine (SVM), artificial neural networks (ANN) and Euclidean distance-based system to classify seven different types of cells. Literature [55] used the fuzzy C-means (FCM) to segment the single cell images and tested on 5 classifiers including Bayesian classifier, linear discriminant analysis (LDA), K-nearest neighbor (KNN), artificial neural networks (ANN), and support vector machine

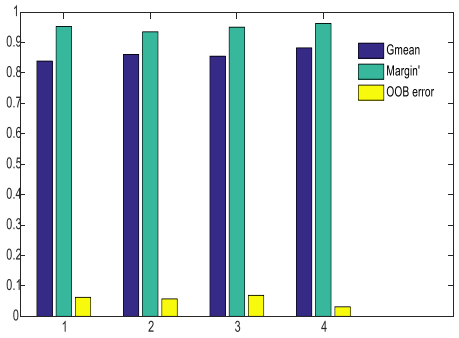

FIGURE 12. Comparison of random forest classifier under different parameter configurations.

TABLE 11. Comparison of results using improved and common random forest classifier.

Index / Model	1	$\sqrt{M}$	$\log_2 M+1$	AFSA-RF
nTree	150	150	150	**273**
k	1	3	4	**3**
Attribute	10	10	10	**6**
G-mean	0.8390	0.8609	0.8551	**0.8824**
Margin	0.9528	0.9352	0.9604	**0.9627**
OOB error	0.0625	0.0574	0.0690	**0.0314**

(SVM) with nucleus-based and cell-based features. Among the 4 methods, the accuracy of literature [53] is 80.92% and the number of features is 11. The recognition accuracy of this paper is 0.4% higher and the number of features is reduced by 2. As for literature [52] and [55], it is concluded that the recognition effect may not behave well with a larger number of features. However, literature [54] and [55] adopted 9 features, while the recognition accuracy was not as high as the algorithm proposed in this paper, which was 4.64% and 1.73% lower respectively. Therefore, feature selection methods do not only reflect differences among cells, high recognition accuracy of which also counts a lot. In view of the recognition accuracy and feature number among 5 kinds of feature selection algorithms, the method proposed in this paper can achieve higher accuracy with a smaller feature number, which is of great value for cell classification and recognition.

From the feature extraction experiment above, we have built the relation between the cell biological characteristics and the features of computer graphics. Since the description of cells is no longer limited to non-quantitative characterization, but accurately embodied in properties of chroma, shape, texture, etc. This also makes it possible to establish a cell feature evaluation system based on computer graphics, no matter what period cells stay, whether they are normal or not, a clear quantitative index is established to provide multi-dimensional feature judgment.

C. CLASSIFIER ANALOGY EXPERIMENT

1) CLASSIFIER ANALOGY EXPERIMENT

The purpose of this experiment is to verify the validity of the random forest classifier based on artificial fish swarm algorithm. The applied data have been introduced in Table 2 and Figure 2. All the data are selected to ensure that the classifier is not inclined to any one part. They have also been checked by our pathologists aiming at ensuring the accuracy of the data. Experimental process is shown as below:

Firstly setting the parameters of the classifier $popsize = 10$, $\max gen = 20$, $try\_number = 6$, $\delta = 0.62$, $visual = 3$. Comparison between the RF classifiers using parameter optimization and the classifiers without parameter optimization on the main indicators including classification margin, geometric mean (G-mean) and OOB error are shown in Table 11. Classifiers with different characters will behave differently in application, they can complement each other and cover weaknesses of the others, especially when they are diverse enough. In this part we modify the parameter of each classifier and observe its performance in classification, which will all contribute to the results. Among the results in Table 11, the *nTree* value of random forest classifiers without parameter optimization is 150, meanwhile,the k value is set as $1, \sqrt{M}$, and $\log_2 M + 1$, which are also compared by histogram in Figure 12.

Compared with the random classifier, G-mean value of the random forest classifier after the optimization is small, while the margin value of the former one is obviously higher than the latter, and the OOB error gets smaller. It is concluded that the base classifier of optimized random forest classifier achieves a higher confidence on the classification results. The recognition rate of the improved classifier is higher and the generalization ability is stronger.

2) EVALUATION FOR DIFFERENT CLASSIFICATION METHODS

In order to illustrate the superiority of the classification method proposed in this paper, we decided on five mostly used classification parameters to compare the improved random forest model with the others, which are accuracy (ACC), sensitivity (SEN), specificity (SPE), positive predictive value (PPV) and negative predictive value (NPV). Relevant results have been shown in Table 12. It should be noted that the accuracy calculation method in this part adopts the proportional weighted calculation method for different kinds of data, including normal epithelial cells, cancerous epithelial cells and so on, which comprehensively describes the classification performance of this method in various kinds of cell data.

In regards to verify the performance of the proposed method in this paper, several methods already used by other researchers in cell classification, like Bayesian classifier [56], KNN [57], and SVM with different kernels [58], Artifact classifier + 4 Iterative Abnormality MLP classifiers [59], Gabor feature-based algorithm [60] are introduced for comparison. Fivefold cross-validation method is used to calculate the accuracy aiming at guaranteeing the effectiveness of the

TABLE 12. Accuracy of proposed method in 2 and 7 classifications.

Accuracy	2 classification (%)	7 classification (%)
ACC	96.86	96.71
SEN	96.79	96.45
SPE	98.14	97.98
PPV	99.53	98.55
NPV	99.07	98.49

TABLE 13. Comparison with other methods on 2 classifications.

Methods	Accuracy (%)	Sensitivity (%)	Specificity (%)
REF [52]	86.78	91.79	91.30
REF [51]	89.39	80.49	81.82
REF [55]	93.7	/	/
REF [21]	94.3	88.1	100
REF [56]	96.10	94.25	93.45
AFSA-RF	**96.86**	**96.79**	**98.14**

TABLE 14. Comparison with other methods on 7 classifications.

Methods	Accuracy (%)	Sensitivity (%)	Specificity (%)
REF [51]	73.28	94.96	66.53
REF [57]	68.48	84.15	84.71
REF [53]	85.39	94.22	92.56
REF [55]	67.25	65.48	87.19
AFSA-RF	**96.71**	**96.45**	**97.98**

contrast experiment. Based on the experimental data, 2 and 7 classifications were applied respectively. 2 classifications refer to dividing cells into normal cells and cancer cells, 7 classifications refer to classify the cell into superficial squamous, intermediate squamous, columnar, mild dysplasia, moderate dysplasia, severe dysplasia, and carcinoma in situ. Dataset contains samples of various types of cells and is accurately classified according to pathologists' notes to ensure the accuracy of the data. Comparative results are as shown in the Table 13 and 14.

As is shown in Table 13, it is concluded that AFSA-RF can achieve better accuracy. Sensitivity and specificity were also higher. The average accuracy of the other five methods cited in Table 13 is 92.05%, the accuracy of the method proposed in this paper is 4.81% higher than that. Although the specificity of the proposed method is not the highest, REF [59] reaches a level of 100%, the accuracy of the proposed one is higher than REF [59]. Accuracy is a more important parameter in the field of cervical cell classification, so the method presented here is a little superior.

In regards to the 7 classifications, the superiority of the AFSA-RF algorithm is more obvious, which behaves better than that of 2 classification on accuracy, sensitivity and specificity. The average accuracy of the other 4 methods only reaches to 73.6%, with a maximum of 85.39%. AFSA-RF algorithm shows 23.11% higher than the average value, it also increases 11.32% comparing with the maximum. As for the sensitivity, the average value of the other 4 methods reaches 92.20%, the max value is 94.96%. The sensitivity value of AFSA-RF is 4.25% and 1.49% better than the average and max value. The specificity of average and max value also improves 15.23% and 5.42%, respectively.

From the experiments narrated above, it is concluded that the AFSA-RF classification method behaves better on accuracy, sensitivity and specificity comparing with other algorithms. By which the superiority of the proposed method is illustrated.

Besides, we also introduced the lymphocyte, normal epithelial cells as well as cancerous epithelial cells under the 2 classifications, fivefold cross-validation to calculate the recognition rate of different classifiers, comparing with SVM and KNN. Relevant results are shown in Table 15.

TABLE 15. Comparison of improved random forest and SVM, KNN.

Recognition rate of classifier (%)				
Type of cell	cell number	SVM	KNN	AFSA-RF
A	400	87.14	86.67	**95.45**
B1	200	91.03	91.26	**98.43**
B2	200	91.72	92.96	**98.11**

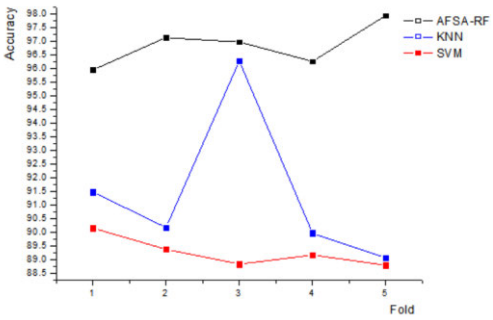

FIGURE 13. Comparison with KNN, SVM on cell level dataset (2 classification.

In the Table 15, the capital letter A stands for lymphocyte, B1 stands for normal epithelial cells and B2 stands for cancerous epithelial cells. From the Table 15 it is concluded that as for A, B1 and B2 the improved random forest algorithm (AFSA-RF) behaves better than SVM and KNN, especially when detecting B2 which stands for cancerous epithelial cells and this is vital for the diagnosis and treatment of cervical cancer.

3) CROSS-VALIDATION AT THE CELL AND SMEAR LEVELS

The proposed method was compared with 2 existing methods aiming at have a fair comparison using the same dataset. Our approach and the other 2 methods (SVM, KNN) were tested on the database generated in this paper. Results are displayed in the Figure 13, 14 and 15. The method of 2 and 7 classification as well as fivefold method were also used to calculate the accuracy.

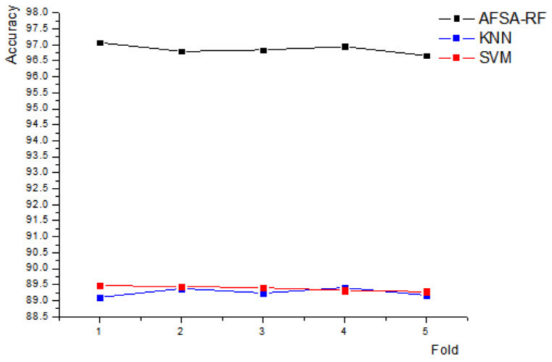

FIGURE 14. Comparison with KNN, SVM on cell level dataset (7 classification).

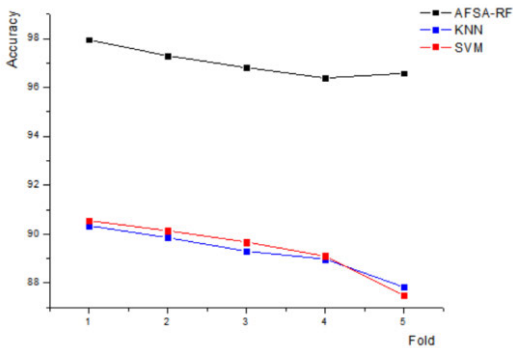

FIGURE 15. Comparison with KNN, SVM on smear level dataset (2 classification).

As is shown in Figure 13 and 14, the method proposed in this paper achieves better performance and higher accuracy, which is proved to be superior in cell classification under 2 and 7 classification.

Accuracy calculated on smear level is as is shown in Figure 15. It is concluded that curve trend of different classification methods is relatively smooth. Compared with the traditional SVM and KNN methods, the method in this paper still has certain advantages in accuracy. All results indicate that the method is promising in the classification of cervical cells, which also removes observer bias and improves efficiency.

4) COMPARISON OF THE TIME COST ON SAME CLASSIFICATION TASK

In order to observe the processing time of different classification methods, we set a fixed classification task, which is to classify 15 normal epithelial cells, 15 positive epithelial cells and 10 lymphocytes. The efficiency of the classifiers can be directly verified by observing the processing time of classifiers on the same data. Results are as shown in Table 16. We adopted SVM, KNN and the proposed algorithm as classifiers in this paper. Hardware environment is Intel 8 generation i7 processor with a memory of 16GB, running in the environment of Win10 system.

The time that takes to achieve the classification target is as shown above. Time consumption of the proposed method is reduced by about 25.6s and 21s comparing with SVM and KNN, respectively, which effectively improves the speed of cell classification.

TABLE 16. Comparison of time cost to achieve classification.

Time	Normal cells (s)	Cancer cells (s)	Lymphocytes (s)	Total (s)
SVM	102.1	88.5	38.3	228.9
KNN	97.5	79.5	32.4	209.4
AFSA-RF	**76.5**	**70.5**	**28.1**	**175.1s**

5) BIOLOGICAL ENLIGHTENMENT FROM ANALOGICAL EXPERIMENTS

Classifier analogy experiment mainly reflects the classifier index and results under different circumstances. As is shown, the optimized classification model achieves a better performance comparing with the other methods. The weight of different cell features in the classification can be clearly displayed, which provides standards for classifications as well as medical teaching. Different characteristics like G-mean, margin, and OOB error will provide references for the optimization of biological cell recognition, which may even reveal the potential relationship between different types of cells in function and differentiation during the classification process.

VII. SUMMARY

This paper introduced the AFSA based random forest algorithm for cervical cell classification. The proposed method applied block Otsu and SVF Snake model to separate and segment epithelial cells and lymphocytes accurately. Chroma, shape and texture features of cells are extracted for classification. Feature selection algorithm based on AFSA is applied to get the optimal feature set, respectively. AFSA based random forest method is used as the classifier. The classification results show that the selected features can significantly distinguish different cell images including abnormal and impurities. The AFSA based random forest classifier have better classification performance than the other common methods, including time cost and accuracy. We demonstrate the promise of this algorithm for improving cervical cancer diagnosis through its feature selection method and AFSA based classifier. Especially its potential in detecting abnormal cells from normal cells.

VIII. COMPLIANCE WITH ETHICAL STANDARDS

Funding: This work was supported by the Guangdong YiZhiYun Pathologist Group Management Co., Ltd. The fund of this article comes from the cooperative company, which does not belong to the fund support, so there is no relevant grant number.

Conflict of Interest: The authors declared that they have no conflicts of interest to this work. We declare that we do not

have any commercial or associative interest that represents a conflict of interest in connection with the work submitted.

Ethical approval: All procedures performed in studies involving human participants were in accordance with the ethical standards of the institutional and/or national research committee and with the 1964 Helsinki declaration and its later amendments or comparable ethical standards.

Informed consent: Informed consent was obtained from all individual participants included in the study.

REFERENCES

[1] [Online]. Available: http://www.who.int/en/
[2] [Online]. Available: http://www2.cdstm.cn/kpqk/art_detail19c9.html?recno=296237
[3] P. Olusola, H. N. Banerjee, J. V. Philley, and S. Dasgupta, "Human papilloma virus-associated cervical cancer and health disparities," *Cells*, vol. 8, no. 6, p. 622, 2019.
[4] [Online]. Available: http://www.people.com.cn/GB/14739/14742/21478/3076893.html
[5] F. Vafaee, C. Diakos, M. B. Kirschner, G. Reid, M. Z. Michael, L. G. Horvath, H. Alinejad-Rokny, Z. J. Cheng, Z. Kuncic, and S. Clarke, "A data-driven, knowledge-based approach to biomarker discovery: Application to circulating microRNA markers of colorectal cancer prognosis," *npj Syst. Biol. Appl.*, vol. 4, no. 1, p. 20, Dec. 2018.
[6] P. Ming, *A Brilliant Monument*. Beijing, China: Writers Publishing House, 2016, p. 423.
[7] [Online]. Available: http://wjw.sz.gov.cn/jksz/sjfb/mqrkyss/
[8] M. H. Stoler, "Advances in cervical screening technology," *Mod. Pathol.*, vol. 13, no. 3, pp. 275–284, Mar. 2000.
[9] L. Han, "Recognition of precancerous lesions based on deep learning and cervical image," Nanchang Hangkong Univ., Nanchang, China, Tech. Rep., 2019.
[10] J. B. De Tomasi, M. M. Opata, and C. N. Mowa, "Immunity in the cervix: Interphase between immune and cervical epithelial cells," *J. Immunol. Res.*, vol. 2019, pp. 1–13, Apr. 2019, doi: 10.1155/2019/7693183.
[11] C. Bergmeir, M. G. Silvente, and J. M. Benítez, "Segmentation of cervical cell nuclei in high-resolution microscopic images: A new algorithm and a Web-based software framework," *Comput. Methods Programs Biomed.*, vol. 107, no. 3, pp. 497–512, Sep. 2012.
[12] R. L. Cahn, R. S. Poulsen, and G. Toussaint, "Segmentation of cervical cell images," *J. Histochem. Cytochem.*, vol. 25, no. 7, pp. 681–688, 1977.
[13] H. Borst, W. Abmayr, and P. Gais, "A thresholding method for automatic cell image segmentation," *J. Histochem. Cytochem.*, vol. 27, pp. 180–187, 1979.
[14] C.-W. Chang, M.-Y. Lin, H.-J. Harn, Y.-C. Harn, C.-H. Chen, K.-H. Tsai, and C.-H. Hwang, "Automatic segmentation of abnormal cell nuclei from microscopic image analysis for cervical cancer screening," in *Proc. IEEE 3rd Int. Conf. Nano/Mol. Med. Eng.*, Tainan, Taiwan, Oct. 2009, pp. 77–80.
[15] H.-S. Wu, J. Gil, and J. Barba, "Optimal segmentation of cell images," *IEE Proc.-Vis., Image, Signal Process.*, vol. 145, no. 1, pp. 50–56, 1998.
[16] M. E. Plissiti, C. Nikou, and A. Charchanti, "Combining shape, texture and intensity features for cell nuclei extraction in pap smear images," *Pattern Recognit. Lett.*, vol. 32, no. 6, pp. 838–853, Apr. 2011.
[17] P. Malm and A. Brun, "Closing curves with Riemannian dilation: Application to segmentation in automated cervical cancer screening," in *Advances in Visual Computing* (Lecture Notes in Computer Science). Berlin, Germany: Springer, 2009, pp. 337–346.
[18] M.-H. Tsai, Y.-K. Chan, Z.-Z. Lin, S.-F. Yang-Mao, and P.-C. Huang, "Nucleus and cytoplast contour detector of cervical smear image," *Pattern Recognit. Lett.*, vol. 29, no. 9, pp. 1441–1453, Jul. 2008.
[19] C.-H. Lin, Y.-K. Chan, and C.-C. Chen, "Detection and segmentation of cervical cell cytoplast and nucleus," *Int. J. Imag. Syst. Technol.*, vol. 19, no. 3, pp. 260–270, Sep. 2009.
[20] P. Bamford and B. Lovell, "Unsupervised cell nucleus segmentation with active contours," *Signal Process.*, vol. 71, no. 2, pp. 203–213, Dec. 1998.
[21] L. Zhang, H. Kong, C. T. Chin, S. Liu, X. Fan, T. Wang, and S. Chen, "Automation-assisted cervical cancer screening in manual liquid-based cytology with hematoxylin and eosin staining," *Cytometry Part A*, vol. 85, no. 3, pp. 214–230, Mar. 2014.
[22] A. Tareef, Y. Song, W. Cai, H. Huang, H. Chang, Y. Wang, M. Fulham, D. Feng, and M. Chen, "Automatic segmentation of overlapping cervical smear cells based on local distinctive features and guided shape deformation," *Neurocomputing*, vol. 221, pp. 94–107, Jan. 2017.
[23] S. Ragothaman, S. Narasimhan, M. G. Basavaraj, and R. Dewar, "Unsupervised segmentation of cervical cell images using Gaussian mixture model," in *Proc. IEEE Conf. Comput. Vis. Pattern Recognit. Workshops (CVPRW)*, Las Vegas, NV, USA, Jun./Jul. 2016, pp. 70–75.
[24] J. Prinyakupt and C. Pluempitiwiriyawej, "Segmentation of white blood cells and comparison of cell morphology by linear and Naïve Bayes classifiers," *Biomed. Eng. OnLine*, vol. 14, no. 1, Dec. 2015, Art, no. 63.
[25] R. R. Kumar, V. A. Kumar, P. N. S. Kumar, S. Sudhamony, and R. Ravindrakumar, "Detection and removal of artifacts in cervical cytology images using support vector machine," in *Proc. IEEE Int. Symp. IT Med. Educ.*, Cuangzhou, China, Dec. 2011, pp. 717–721.
[26] I. A. Yusoff, N. A. M. Isa, N. H. Othman, S. N. Sulaiman, and Y. Jusman, "Performance of neural network architectures: Cascaded MLP versus extreme learning machine on cervical cell image classification," in *Proc. 10th Int. Conf. Inf. Sci., Signal Process. Appl. (ISSPA)*, Kuala Lumpur, Malaysia, May 2010, pp. 308–311.
[27] W. Wanyin, "Research on laser water degradation image restoration algorithm based on model method FDL," Central South Univ., Changsha, China, Tech. Rep., 2013.
[28] J. Zhang and Y. Liu, "Cervical cancer detection using SVM based feature screening," in *Proc. Int. Conf. Med. Image Comput. Comput. Assist. Intervent.*, 2004, pp. 873–880.
[29] T. Chankong, N. Theera-Umpon, and S. Auephanwiriyakul, "Cervical cell classification using Fourier transform," in *Proc. ICBME*, 2008, pp. 476–480.
[30] Y.-F. Chen, P.-C. Huang, K.-C. Lin, H.-H. Lin, L.-E. Wang, C.-C. Cheng, T.-P. Chen, Y.-K. Chan, and J. Y. Chiang, "Semi-automatic segmentation and classification of pap smear cells," *IEEE J. Biomed. Health Informat.*, vol. 18, no. 1, pp. 94–108, Jan. 2014.
[31] L. J. Mango, "Computer-assisted cervical cancer screening using neural networks," *Cancer Lett.*, vol. 77, nos. 2–3, pp. 155–162, Mar. 1994.
[32] Y. Marinakis, M. Marinaki, and G. Dounias, "Particle swarm optimization for pap-smear diagnosis," *Expert Syst. Appl.*, vol. 35, no. 4, pp. 1645–1656, Nov. 2008.
[33] K. Bora, M. Chowdhury, L. B. Mahanta, M. K. Kundu, and A. K. Das, "Pap smear image classification using convolutional neural network," in *Proc. 10th Indian Conf. Comput. Vis., Graph. Image Process. (ICVGIP)*, Guwahati, India, Dec. 2016, pp. 55:1–55:8.
[34] J. Su, X. Xu, Y. He, and J. Song, "Automatic detection of cervical cancer cells by a two-level cascade classification system," *Anal. Cellular Pathol.*, vol. 2016, pp. 1–11, May 2016.
[35] M. Zhao, L. Chen, L. Bian, J. Zhang, C. Yao, and J. Zhang, "Feature quantification and abnormal detection on cervical squamous epithelial cells," *Comput. Math. Methods Med.*, vol. 2015, pp. 1–9, Mar. 2015.
[36] S. Y. Park, D. Sargent, R. Wolters, and R. W. Lieberman, "Semantic image analysis for cervical neoplasia detection," in *Proc. IEEE 4th Int. Conf. Semantic Comput.*, Sep. 2010, pp. 160–165.
[37] G. H. B. Miranda, J. Barrera, E. G. Soares, and J. C. Felipe, "Structural analysis of histological images to aid diagnosis of cervical cancer," in *Proc. 25th SIBGRAPI Conf. Graph., Patterns Images*, Aug. 2012, pp. 316–323.
[38] G. Volgareva, L. Zavalishina, Y. Andreeva, G. Frank, E. Krutikova, D. Golovina, A. Bliev, D. Spitkovsky, V. Ermilova, and F. Kisseljov, "Protein p16 as a marker of dysplastic and neoplastic alterations in cervical epithelial cells," *BMC Cancer*, vol. 4, no. 1, p. 58, Dec. 2004.
[39] Y. Liang, Z. Tang, and M. Yan, "Comparison-based convolutional networks for cell/clumps detection in the limited data scenario," Tech. Rep., 2018.
[40] C. Rasche, C. Tiganesteanu, M. Neghina, and A. Sultana, "Cervical nuclei classification: Feature engineering versus deep belief network," in *Medical Image Understanding and Analysis* (Communications in Computer and Information Science). Berlin, Germany: Springer, 2017, pp. 874–885.

[41] N. Dhungel, G. Carneiro, and A. P. Bradley, "Automated mass detection in mammograms using cascaded deep learning and random forests," in *Proc. Int. Conf. Digit. Image Comput., Techn. Appl. (DICTA)*, Adelaide, SA, Australia, Nov. 2015, pp. 1–8.

[42] D. Maji, A. Santara, S. Ghosh, D. Sheet, and P. Mitra, "Deep neural network and random forest hybrid architecture for learning to detect retinal vessels in fundus images," in *Proc. 37th Annu. Int. Conf. IEEE Eng. Med. Biol. Soc. (EMBC)*, Milan, Italy, Aug. 2015, pp. 3029–3032.

[43] S. Bai, "Growing random forest on deep convolutional neural networks for scene categorization," *Expert Syst. Appl.*, vol. 71, pp. 279–287, Apr. 2017.

[44] L. Li, S. Deng, and X. Deng, "Two value algorithm for image segmentation based on the method of Otsu," *Microcomput. Inf.*, no. 14, pp. 76–77, 2005.

[45] X. Bresson, S. Esedoḡlu, P. Vandergheynst, J.-P. Thiran, and S. Osher, "Fast global minimization of the active Contour/Snake model," *J. Math. Imag. Vis.*, vol. 28, no. 2, pp. 151–167, Aug. 2007.

[46] J. Tang, "A multi-direction GVF snake for the segmentation of skin cancer images," *Pattern Recognit.*, vol. 42, no. 6, pp. 1172–1179, Jun. 2009.

[47] R. Díazuriarte and D. A. S. Alvarez, "Gene selection and classification of microarray data using random forest," *BMC Bioinf.*, vol. 7, no. 1, p. 3, 2006.

[48] V. Svetnik, A. Liaw, C. Tong, J. C. Culberson, R. P. Sheridan, and B. P. Feuston, "Random forest: A classification and regression tool for compound classification and QSAR modeling," *J. Chem. Inf. Comput. Sci.*, vol. 43, no. 6, pp. 1947–1958, Nov. 2003.

[49] C. Lindner, P. A. Bromiley, M. C. Ionita, and T. F. Cootes, "Robust and accurate shape model matching using random forest regression-voting," *IEEE Trans. Pattern Anal. Mach. Intell.*, vol. 37, no. 9, pp. 1862–1874, Sep. 2015.

[50] M. Ma, J. Liang, L. Sun, and M. Wang, "SAR image segmentation based on SWT and improved AFSA," in *Proc. 3rd Int. Symp. Intell. Inf. Technol. Secur. Inform.*, 2010, pp. 146–149.

[51] K. Bora, M. Chowdhury, L. B. Mahanta, M. K. Kundu, and A. K. Das, "Automated classification of pap smear images to detect cervical dysplasia," *Comput. Methods Programs Biomed.*, vol. 138, pp. 31–47, Jan. 2017.

[52] M. Zhao, A. Wu, J. Song, X. Sun, and N. Dong, "Automatic screening of cervical cells using block image processing," *Biomed. Eng. OnLine*, vol. 15, no. 1, p. 14, Dec. 2016, doi: 10.1186/s12938-016-0131-z.

[53] T. A. Sajeena and A. S. Jereesh, "Automated cervical cancer detection through RGVF segmentation and SVM classification," in *Proc. Int. Conf. Comput. Netw. Commun. (CoCoNet)*, Dec. 2015, pp. 663–669.

[54] T. Chankong, N. Theera-Umpon, and S. Auephanwiriyakul, "Automatic cervical cell segmentation and classification in pap smears," *Comput. Methods Programs Biomed.*, vol. 113, no. 2, pp. 539–556, Feb. 2014.

[55] E. J. Mariarputham and A. Stephen, "Nominated texture based cervical cancer classification," *Comput. Math. Methods Med.*, vol. 2015, pp. 1–10, Jan. 2015.

[56] P. Wang, L. Wang, Y. Li, Q. Song, S. Lv, and X. Hu, "Automatic cell nuclei segmentation and classification of cervical pap smear images," *Biomed. Signal Process. Control*, vol. 48, pp. 93–103, Feb. 2019.

[57] L. Zhang, L. Lu, I. Nogues, R. M. Summers, S. Liu, and J. Yao, "DeepPap: Deep convolutional networks for cervical cell classification," *IEEE J. Biomed. Health Informat.*, vol. 21, no. 6, pp. 1633–1643, Nov. 2017.

DONGYAO JIA (Senior Member, IEEE) was born in Henan, China, in 1974. He graduated from Tsinghua University, in 2006, and the Ph.D. degree in engineering.

He is currently a Professor and a Ph.D. Supervisor with Beijing Jiaotong University. He has presided or participated in 863 sub-projects, 863 major projects, and major projects of the National Natural Science Foundation, the Science and Technology Support Project of the Ministry of Science and Technology, the third-class Hospital, Metro Corporation, and other engineering and scientific research projects. He has published *Optimization Method for Crop Growth Characteristics Based on Improved Locality Preserving Projection* (*Journal of Applied Mathematics*, 2014), *Reduction of Multidimensional Image Characteristics Based on Improved KICA* (*Journal of Applied Mathematics*, 2014), *Layer-Cluster Topology Sensor Node Deployment for Large-Scale Multi-Nodes of WSN* (Wireless Personal Communications, 2017), *Adaptive Multi-Path Routing Based on an Improved Leapfrog Algorithm* (Information Sciences, 2016). *Recognition Method Based on Green Associative Mechanism for Weak Contrast Vehicle Targets* (Neurocomputing, 2016), *A Control System of Indoor Air Quality Based on Modified Smith Predictor*, (Proceedings, 2010), *CrossStrait Conference on Information Science and Technology*, (Qinhuangdao, China: 2010), and *Metamerism Breakdown Characteristic and its Application in Detection of Foreign Materials* (Spectroscopy and Spectral Analysis, 2008). His main research interests include new detection technology in traffic field, medical image processing, and data mining.

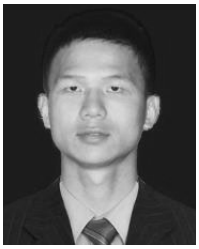

ZHENGYI LI was born in Shandong, China, in 1993. He graduated from the Department of Automation, Beijing Jiaotong University. He received the master's degree in 2018. He joined the National Laboratory of Digital Multimedia, HIKVISION, and worked as a Senior Algorithmic Engineer. His main research interests include medical images detection and recognition and tracking algorithms based on deep learning. His main work is to use deep learning technology to intellectualize traditional household appliances.

CHUANWANG ZHANG was born in Hebei, China, in 1995. He received the bachelor's and master's degrees from Beijing Jiaotong University, where he is currently preparing to pursue the Ph.D. degree. He has been responsible for several cervical cancer and breast cancer detection projects. He used to develop a prototype machine which can be popularized in the market and possessed rich experience in the field of medical image processing. His main research interest includes medical image detection.